The Tilt Angle and Flame Trajectory of Buoyant Jet Diffusion Flames under Upslope and Downslope Wind Conditions

Kong X.X.[1], Wang X.S.[1,*], Zhu P.[2], Liu Y.P.[1], Zhu J.P.[1]

[1] *State Key Laboratory of Fire Science, University of Science and Technology of China, Hefei, China*

[2] *Department of Engineering Physics, Tsinghua University, Beijing, China*

**Corresponding author emails: wxs@ustc.edu.cn, jpzhu@ustc.edu.cn*

ABSTRACT

The tilt angle and flame trajectory of jet diffusion flames under upslope and downslope wind conditions have not been studied before and no data are available in the literature. This paper presents an experimental investigation on the tilt angle and flame trajectory of a round jet diffusion flame under upslope and downslope wind with attack angles from 0° to ±20° and speeds from 0 to 2.45 m/s for downslope wind flow (-) and from 0 to 2.12 m/s for upslope wind flow (+). The tilt angle and flame trajectory are determined based on the luminous intermittency of the flame images. The results show that, at a given wind attack angle for upslope and downslope wind, the flame tilt angle generally increases with the increase of wind speed up to an asymptotic value. At a given wind speed, the flame tilt angle decreases with the increase of wind attack angles. It is also observed that the orientation of wind flow has different effects on the jet flame: for instance, as the wind attack angle increases, the phenomenon of flame downwash occurs at higher wind speeds than under horizontal flow. The flame trajectory in the jet region shows different evolutionary trends under upslope wind and downslope wind, which can be collapsed by normalizing coordinates with the length scale $r^2 d_j$. Moreover, two correlations are developed to predict the tilt angle and flame trajectory of the curved jet diffusion flames under upslope and downslope winds, which are valuable for evaluating fire behavior under different wind conditions.

KEYWORDS: Jet diffusion flame, flame trajectory, tilt angle, upslope, downslope, wind.

NOMENCLATURE

b_f flame width (m)

c_P specific heat (kJ/(kg·K))

d nozzle diameter (m)

g gravitational acceleration (m/s^2)

Fr Froude number (-)

H flame height (m)

ΔH heat of combustion (kJ/kg)

L mean flame length (m)

$\dot{m}$ mass flow rate (kg/s)

$\dot{M}$ momentum (kg·m/s^2)

Q_F flow rate (L/min)

$\dot{Q}$ heat release rate (kW)

T temperature (K)

$A, B, k_h, k_v m, n$ constants in the equations (-)

K_G geometric shape parameter

σ standard deviation

Greek

α, β, γ constants in the equations (-)

θ_f flame tilt angle (°)

ρ fluid density (kg/m^3)

Subscripts

∞ ambient

f fire

Proceedings of the Ninth International Seminar on Fire and Explosion Hazards (ISFEH9), pp. 619-630
Edited by Snegirev A., Liu N.A., Tamanini F., Bradley D., Molkov V., and Chaumeix N.
Published by St. Petersburg Polytechnic University Press
ISBN: 978-5-7422-6496-5 DOI: 10.18720/spbpu/2/k19-56

$\dot{Q}^*$ dimensionless heat release rate (-)
u,V velocity (m/s)
r momentum flux ratio
S stoichiometric mass ratio (-)
j jet
W wind
H horizontal
V vertical

INTRODUCTION

Jet diffusion flames have attracted considerable attention in recent decades, owing to frequent fire and explosion accidents caused by gas leakage in the pipe gallery and numerous practical applications in industries, such as smoke exhaust from refineries and the rapid dissipation of unwanted flammable gas effluent [1, 2]. As a fundamental and practical problem in fire research, jet flame behavior has also been studied extensively, although most research has mainly focused on fire behavior under still or crossflow conditions, where flame height [3-5], flame tilt angle [6-10], flame length [10-14], and flame thermal radiation [18-19] were considered. However, in the actual fire scene, the ambient airflow is complex and changeable, and the oblique airflow frequently occurs. In addition, the fire behavior of gaseous fuel jet flame under oblique wind flow has not been studied before and therefore no data are available in the literature. Therefore, it is still valuable to investigate the flame characteristics of jet diffusion flames under upslope and downslope wind conditions.

Pipkin et al. [6, 7] proposed a flame tilt angle formula to represent the bending degree of the flame, in which a drag coefficient related to the Re was introduced. Oka et al. [8] presented an empirical model based on the balance of mass between the upward hot current and crosswind as $\tan\theta_f \propto Fr_w^m \dot{Q}^{*n}$, which indicated the quantitative relationship between tilt angle and the dimensionless heat release rate and wind Froude number. Wang et al. [9] derived a global flame tilt angle formula in crosswind coupling the influences of buoyancy and inertia force on turbulent flame with a continuous variation in r. Kalghatgi [10] observed the shapes and sizes of hydrocarbon jet diffusion flames in a crosswind flow, and presented empirical models of flame length and tilt angle related to the velocity ratio (u_j/u_w) by describing the flame shape as a cone frustum.

De Faveri et al. [11] presented correlations to predict the flame trajectory lengths of fires with a high-source momentum ($\dot{Q}^* > 1$), which indicated that the flame length is correlated with the source Froude number and the Reynolds number, although the effects of the latter are negligible if the Froude number is less than 0.1. Majeski et al. [12] proposed a phenomenological model to represent the flame length of low-momentum jet diffusion flames in crossflow by employing two basic principles in the flame shape and the flame size. Wang et al. [13] proposed a correlation to describe the flame trajectory-line length in both sub-pressure and normal pressure atmospheres, which was fitted well with the experimental results.

However, the studies of a jet fire described above have been limited to horizontal wind only, with few studies focusing on the effects of upslope and downslope wind flow. Ellzey et al. [17] observed that the orientation of the fuel jet relative to the air wind has a significant effect on the flame shape and the soot yield. The studies by Tao and Zhu et al. [15, 16] considered the effects of oblique wind flow on the ethanol pool fire burning rate, while Zhu et al. [14] considered the flame characteristics, but only a liquid pool fire was investigated, which has a lower initial momentum than a jet fire. The difference of fundamental aspect in the flame tilting between the horizontal wind flow and the oblique wind flow is that there are two momentum components (horizontal and vertical) in the latter. It can be seen that the horizontal momentum component always tends to cause the flame tilt angle to increase, whereas the vertical momentum component tends to help the flame retain its vertical orientation if it is in the same direction as the flame momentum. When the vertical

momentum component and the flame momentum are in opposite direction, i.e., under downslope wind, the vertical momentum component will reduce or counter balance the buoyancy force, and the change in the flame tilt angle will be enhanced. As no data are available in the literature, further studies and quantification are still needed to reveal the manner in which such jet fire behavior would be changed in upslope and downslope wind flow.

Jet fires may in fact occur under changeable airflow conditions and in any terrain, such as upslope and downslope wind, and usually inflict major hazards and risks. For example, gas leakage fire occurring in gas pipelines would be affected by oblique wind, as would fires occurring in a sloped tunnel. In such circumstances, flame characteristics may be influenced by wind speed as well as wind direction, and the deflected flame under upslope and downslope wind conditions may cause more serious thermal damage to neighboring objects and persons. Therefore, the parameters describing the shape of the flame, such as the tilt angle and trajectory, are of great significance for evaluating fire behavior under upslope and downslope wind conditions.

So, a series of experiments was carried out in this study to investigate the effects of upslope and downslope wind flow on the fire behavior of a jet diffusion flame with different wind attack angles and wind speeds, in which the tilt angle and trajectory of the jet flame were quantitatively determined and analyzed. New correlations were then proposed to correlate the flame tilt angle and trajectory with wind attack angles.

THEORETICAL ASPECTS

The majority of experimental scenarios demonstrates that the visual tips of the deflected flame are located below the tunnel ceiling under downslope wind flows. It means that the flame body under downslope wind flows can simply move upwards in the wind tunnel, without touching the ceiling in this study.

In order to model such a jet diffusion flame, certain assumptions are required regarding its body shape. The flame body shape has been modeled to be a frustum of a cone at larger velocity-ratio value u_f/u_w (greater than 4) [10]. The experiments indicate that the half cone angle for the frustum is small and varies from a value of about 2.8° to 5° with the variation in u_j/u_w. In this study, the velocity-ratio value $u_f/u_w < 4$ when $u_w > 0.4$ m/s, which indicates that the cylindrical shape model is more suitable for the jet flame being tested with wind speeds ranging from 0.4 to 2.45 m/s when $u_w > 0.4$ m/s in this study.

Moreover, the flame body shape is supposed to be geometrically similar, which requires that the flame width b_f change in proportion to the flame length L_f with the geometric shape parameter K_G that may be dependent on the airflow conditions as $b_f = K_G L_f$ [9, 12]. Furthermore, the combustion efficiency of a propane diffusion flame is assumed to be 100%. Based on the investigation by Kostiuk et al. [20-21], this hypothesis is supported because the combustion efficiency of a propane diffusion flame is insensitive to crosswind within the considered range, where the lowest combustion efficiency would be 99%.

As illustrated in Fig. 1, the flame tilt angle θ_f is assumed to be controlled by the momentum balance of the horizontal $\dot{M}_H$ and vertical $\dot{M}_V$ direction at the average flame height. When the flame body is regarded as the control volume, the tilt angle of the flame body can be represented based on the momentum balance equation in the normal direction of the flame surface as $\tan\theta_f = \dot{M}_H / \dot{M}_V$, where $\dot{M}_H = \dot{m}_H V_H$ and $\dot{M}_V = \dot{m}_V V_V$, respectively.

In order to simplify the analysis, we assume that the effects of the horizontal ($u_H = u_w \cos\theta_w$) and vertical ($u_V = u_w \sin\theta_w$) velocity components of the oblique wind u_w on the axial fuel velocity are

considered individually. Corresponding to the two velocity components, the wind Froude number Fr_w should also contain horizontal and vertical components, namely $Fr_H = u_H^2/gd_j = (u_w\cos\theta_w)^2/gd_j$ and $Fr_V = u_V^2/gd_j = (u_w\sin\theta_w)^2/gd_j$.

In the horizontal direction, the mass flow rate of the horizontal velocity component u_H flowing through the cylindrical flame surface is [9]:

$$\dot{m}_H = \rho_\infty u_H b_f L\cos\theta_f = \rho_\infty u_H K_G L^2\cos\theta_f, \tag{1}$$

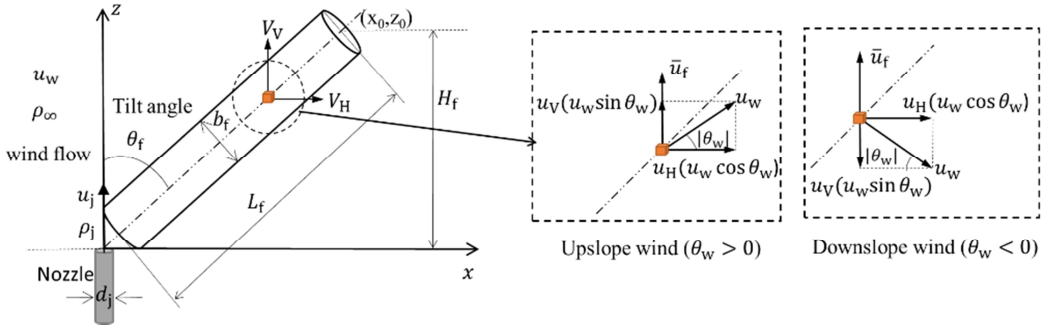

Fig. 1. Definitions of coordinates x, z, velocity components, width b_f, flame trajectory (x_0,z_0) and tilt angle θ_f under upslope and downslope wind.

In the vertical direction, the mass flow rate can be determined by the vertical velocity component ($\dot{m}_v$) and stoichiometric mixture ($\dot{m}_f$):

$$\dot{m}_v = \rho_\infty u_V b_f L\sin\theta_f = \rho_\infty u_V K_G L^2\sin\theta_f, \tag{2}$$

$$\dot{m}_f = (S+1)\dot{m}_j = 0.25\pi(S+1)\rho_j u_j d_j^2, \tag{3}$$

where $\dot{m}_j$ is the jet flame mass flow rate and S is the stoichiometric mass ratio of air and fuel for stoichiometric combustion.

Under upslope winds ($\theta_w > 0°$), u_V has the same direction as $\bar{u}_f$, where $\bar{u}_f$ is the mean flame velocity at the average vertical height H_f. Thus, the momentum in the vertical direction can be expressed as $\dot{M}_V = \dot{m}_f\bar{u}_f + \dot{m}_v u_V$. In order to eliminate the discontinuity of the tangent function when covering 90°, θ_f, which is bounded as $\theta_f \le (90° + \theta_w)$, is transformed by 90°, so the tangent function is modified as $\tan(90°-\theta_f)$, i.e.,

$$\tan(90^\circ-\theta_f) = \frac{\dot{M}_V}{\dot{M}_H} = \frac{\dot{m}_f\bar{u}_f}{\dot{m}_H u_H} + \frac{\dot{m}_v u_V}{\dot{m}_H u_H}, \tag{4}$$

When $\theta_w = 0°$, $u_V = 0$ m/s, Eq. (4) is equivalent to the crossflow condition. Based on the previous research [6-9, 22], the flame tilt angle in crosswind can mainly be determined by the dimensionless heat release rate $\dot{Q}^*$ and source Froude number Fr_j, which is based on the momentum balance of the airflow and flame flow, where the $\dot{Q}^*$ is expressed as $\dot{Q}^* = \dot{Q}\Big/\left(\rho_\infty c_P T_\infty\sqrt{gd_j}d_j^2\right)$, while $\dot{Q} = \rho_j u_j d_j^2\Delta H\pi/4$ [23]. Thus, we can obtain,

$$\dot{Q}^* \propto u_j \Big/ \sqrt{d_j} \propto Fr_j^{1/2}, \tag{5}$$

Combining Eq. (5) with the flame tilt angle model proposed elsewhere as $\tan\theta_f \propto Fr_w^m \dot{Q}^{*n}$ [8], the flame tilt angle in crossflow conditions can be expressed as,

$$\tan\theta_f \propto Fr_w^m Fr_j^{n/2}, \tag{6}$$

Associating Eqs. (1), (3), and (6) with Eq. (4) and using the quadratic formula, the simplified tilt angle under upslope and downslope wind can be approximately expressed as,

$$\tan\left(90^\circ - \theta_f\right) = K_h Fr_H^m Fr_j^{n/2} + K_v \tan\theta_w, \tag{7}$$

where the values of the coefficients K_h, K_v, m, n can be obtained by means of regression. Equation (7) also applies to the downslope wind condition ($\theta_w < 0°$).

EXPERIMENTAL SETUP

All experiments were conducted in a small-scale wind tunnel, as presented schematically in Fig. 2, which has a cross-section of 0.6 m wide and 0.42 m high.

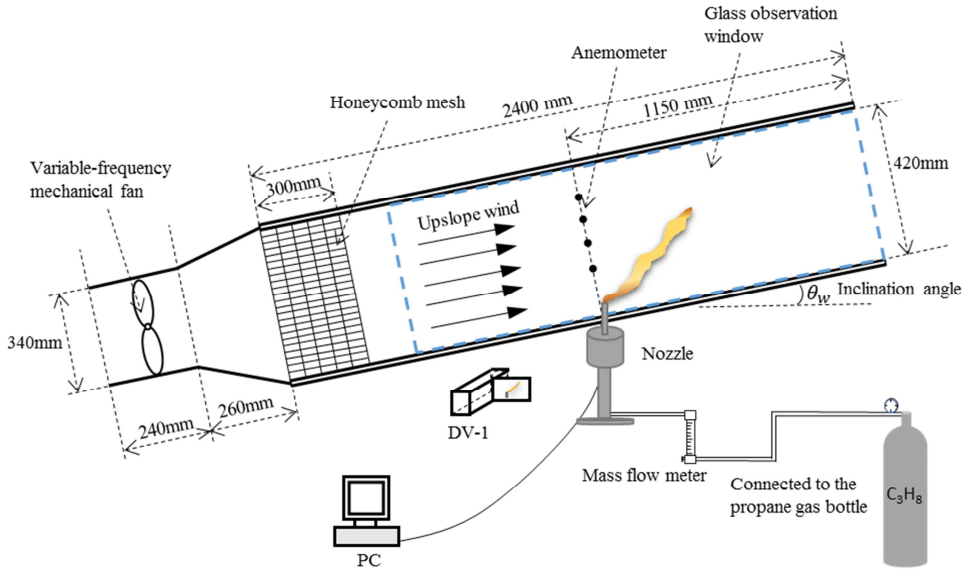

Fig. 2. Schematic of experimental setup.

The wind flow was generated by a two-way axial wind fan, and then passed through the rectifying mesh, which was set at a distance of 0.95 m from the nozzle center in order to minimize the fan disturbance. The uniform and stable air flow speed ranged from 0 to 2.45 m/s for downslope wind flow and from 0 to 2.12 m/s for upslope wind flow at the test section. The instantaneous wind speed flowing across the test section was monitored by four-probe hot-wire anemometers prior to fuel ignition. The jet diffusion flames were established at the exits of circular stainless steel nozzles with inner diameters of 4, 6, 8 and 10 mm. The nozzle tip was approximately 0.07 m above the tunnel floor in order to locate any flame outside the tunnel wall boundary layers. The fuel (C_3H_8 with 99.99% purity) was supplied from the compressed gas cylinders and controlled by a calibrated mass flow meter with an accuracy of ± 0.8% of reading. The range of fuel exit velocities was 0.05–1.77

m/s with a Reynolds number (Re) of 126–3920, and Froude number (Fr_j) of 0.03–64.7. The ambient air pressure was 1 atm, the temperature was 292.15 K, and the air humidity was approximately 40%. The flame Froude number, $Fr_f = u_j \Big/ \left(\left(g d_j \right)^{1/2} (S+1)^{3/2} \left(\rho_j / \rho_\infty \right)^{1/4} \left(\Delta \overline{T}_f / T_\infty \right)^{1/2} \right)$, was within a range from 0.001 to 1, which is below the threshold value of 5 for a momentum controlled jet fire [4]. Therefore, all the flames tested in the experiments are buoyancy controlled.

All the test cases are described in detail in Table 1. The data are recorded for a duration of 3 min for each experimental condition. All the experiments were repeated 3 times under each scenario and each repeated test was conducted after the wind tunnel and nozzles returned to the initial ambient conditions. The quantitative results presented in this paper are the ensemble average of all the repeated tests. The uncertainties according to the repeats of the experiments are reflected by the error bar of the data presented in the figures.

A method based on flame intermittency image analysis [26] was used to determine the flame trajectory and tilt angle quantitatively from a flame image sequence recorded with a digital camera during the steady stage of combustion. The flame tilt angle caused by winds is usually defined as the angle formed by the vertical direction and the straight line connecting the burner exit centerline and flame tip. Furthermore, the flame trajectory is represented by the position of the flame tip where the probability of flame occurrence is 0.5 [26], as illustrated in Fig. 3.

Table 1. Summary of experimental scenarios

Test cases	Wind attack angle θ_w (°)	Nozzle diameter d_j (mm)	Flow rate Q_F (L/min)	Wind speed u_w (m/s)
Upslope wind	+0/10/15/20	4/6/8/10	0.80/1.20/1.60/2.00	0/0.14/0.25/0.36/0.51/0.7/ 0.86/1.07/1.33/1.59/2.12
Downslope wind	-0/10/15/20	4/6/8/10	0.24/0.80/1.20/2.00	0/0.25/0.38/0.57/0.77/0.9 5/1.20/1.51/1.83/2.45

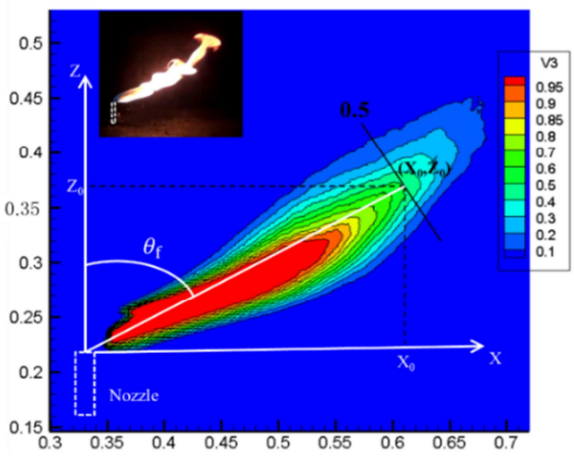

Fig. 3. Quantification of flame trajectory (x_0, z_0) and tilt angle (θ_f) by flame intermittency of 0.5.

RESULTS AND DISCUSSION

Physical appearance of flame

Figure 4 illustrates typical flame images with an increasing wind flow speed at different wind attack angles. It should be noted that all the flames in the experiments are non-lifted with a low momentum, which may result in the occurrence of the wake-trapped behavior near the nozzle. As the flames being tested are stabilized in the near wake region, they are primarily dominated by the complicated aerodynamic interactions among the wind flow, fuel nozzle, and deflected fuel jet.

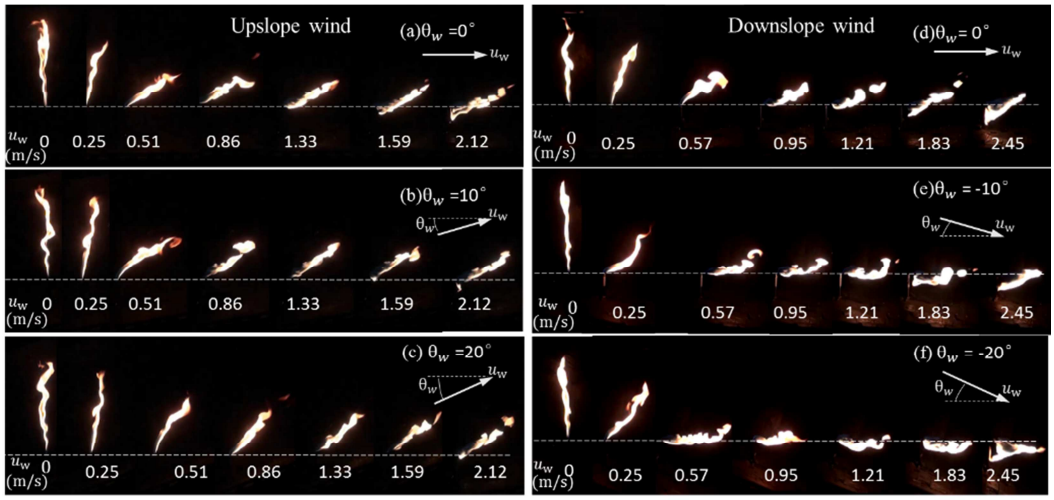

d_j=4mm，u_j=1.59m/s，100KPa

Fig. 4. Typical flame images with an increasing wind flow speed at different wind attack angles.

It can be observed that, during the initial stage (with relatively low wind flow speeds), the upward flow in the lee side of the burner and jet causes a small angle [9] and an elongated flame compared to the cases without wind. At a given wind attack angle, the absolute curvature of the flame becomes more prominent with an increasing wind flow speed, particularly under downslope wind with relatively large oblique directions. At a given wind speed, the flame tilt angle increases with the increase of wind attack angle for downslope airflow, but decreases with the increase of upslope airflow angle. Figure 4 also shows that the flame behavior is more stable for upslope wind than under downslope wind.

Meanwhile, the luminous flame base gradually moves to the lee side of the nozzle. As the wind attack angle ($|\theta_w|$) increases, the flames become more unstable and expand to the downstream area at a large angle. As the absolute flame bending degree becomes nearly parallel to the horizontal direction under relatively strong wind flow; that is, around $u_w \geq 1.83$ m/s for downslope wind, flame downwash occurs, and the downwash areas become larger when the wind speed increases. For upslope wind, as the wind attack angle increases, the phenomenon of flame downwash occurs at higher wind speeds than under horizontal flow. For instance, flame downwash occurs for $u_w \geq 1.59$ m/s at $\theta_w = 0°$, but it occurs for $u_w = 2.12$ m/s when $\theta_w = 10°$ and 20°. Quantitative results are presented in the following subsections.

The typical variations of instantaneous flame tilt angle for sequential flame images under upslope and downslope airflow are shown in Fig. 5. As observed in the instantaneous flame images, there is flame surface fragmentation and the flame position fluctuates with time, causing intermittent flame within the unburnt fuel region. Instantaneous flame tilt angle of sequential flame images in Fig. 5 can be calculated to obtain the average tilt angle of the flame and the standard deviation (σ).

Results show that the standard deviation is within 10%, which can also be reflected in the error bar of the average data recorded with a duration time of 3 min in the figures.

Flame tilt angle

Figure 6 shows the variations of flame tilt angle under different wind speeds and attack angles. It can be seen that, for a certain burner size, the flame tilt angle increases with an increase in wind speed and tends to approach (90° + θ_w) asymptotically. At a given wind speed, θ_f increases with an increase in the wind attack angle $|\theta_w|$ for downslope wind, but decreases for upslope wind. It also shows that the flame tilt angle for a large nozzle diameter d_j reaches nearly parallel to the wind direction at a lower wind speed than for a smaller nozzle diameter. At a given flow rate, the flame for a larger nozzle diameter would have a smaller initial momentum, which results in more obvious bending of the flame than for a smaller nozzle at the same wind speed. However, the growth rate of the tilt angle would diminish with an increase in wind speed. The quantitative trends of flame tilt angle are consistent with the observations as shown in Fig. 4.

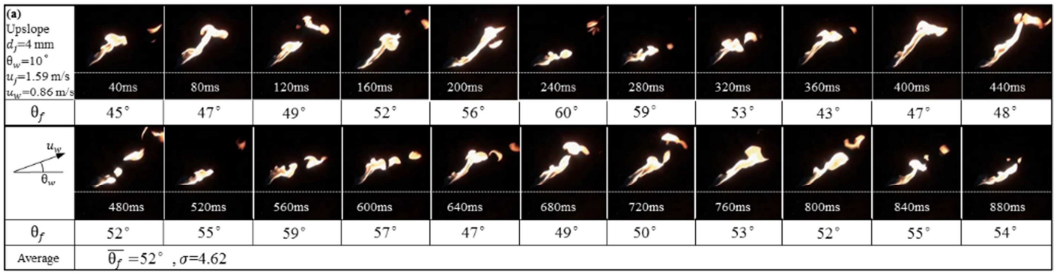

(a) Upslope airflow: d_j = 4 mm, θ_w = 10°, u_j = 1.59 m/s, u_w = 0.86 m/s.

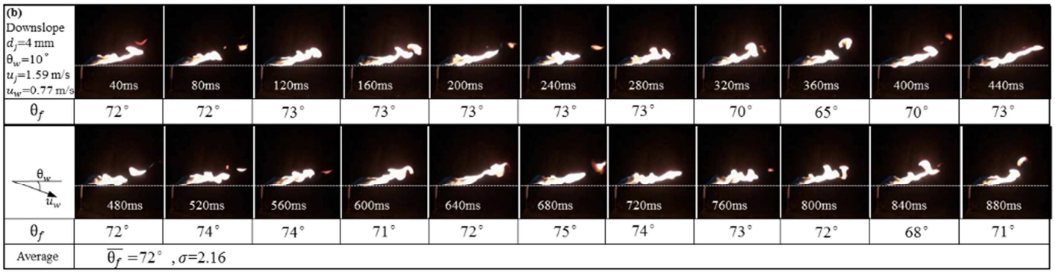

(b) Downslope airflow: d_j = 4 mm, θ_w = 10°, u_j = 1.59 m/s, u_w = 0.77 m/s.

Fig. 5. Sequential flame images of the instantaneous flame.

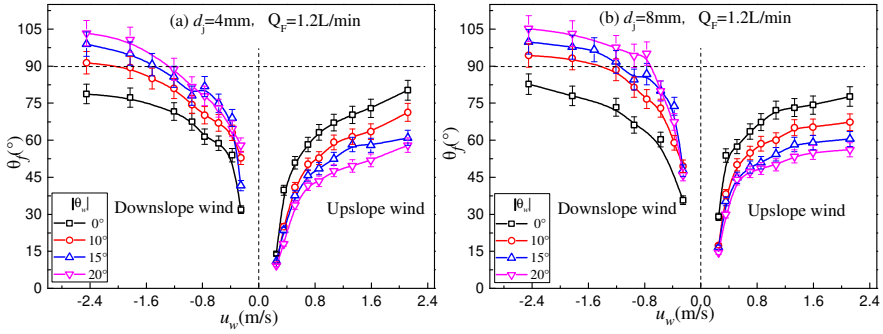

Fig. 6. Flame tilt angle variations with increasing wind flow speeds and attack angles.

Based on the above theoretical analysis, it can be seen that the flame tilt angle can be described by Eq. (7). As illustrated in Fig. 7 (a), by plotting $\tan(90° - \theta_f)Fr_j^{-2/15}Fr_H^{2/5}$ versus $\tan\theta_w Fr_j^{-2/15}Fr_H^{2/5}$ for the cases with all different oblique wind, we can obtain the intercept K_h and the slope ($-K_v$) of the correlation. The proposed correlation takes the following form:

$$\tan\left(90^\circ - \theta_f\right) = 0.94 Fr_j^{2/15} Fr_H^{-2/5} + 1.25\tan\theta_w, \tag{8}$$

The correlation coefficient, R^2, is approximately 0.96 for upslope wind and 0.95 for downslope wind for all of the cases with $|\theta_w|$ = 0°, 10°, 15°, and 20°.

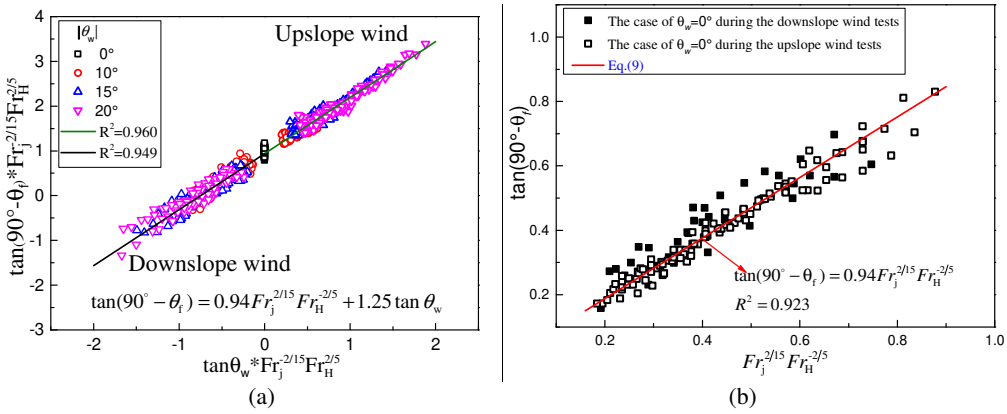

Fig. 7. Correlation results under upslope and downslope wind tests: (a) $|\theta_w| \geq 0^\circ$; (b) $\theta_w = 0^\circ$.

The correlation in Eq. (8) can be a good representation of the change of flame tilt angle variation with different wind attack angles within the specified ranges of the relevant dimensionless group $-2.0 \leq \tan\theta_w Fr_j^{2/15} Fr_H^{-2/5} \leq 2.0$, which is appropriate for $\theta_f \geq 40°$ in this study.

Particularly, when the jet flame is affected by crossflow (θ_w = 0°), $\tan\theta_w$ will be zero. For this case, Eq. (8) can be simplified as:

$$\tan\left(90^\circ - \theta_f\right) = 0.94 Fr_j^{2/15} Fr_H^{-2/5}, \tag{9}$$

which takes the same form as that previously presented [8]. As an applicable example of Eq. (9), Fig. 7 (b) illustrates that the correlation of $\tan(90° - \theta_f)$ versus $Fr_j^{2/15}Fr_H^{-2/5}$ can express the experimental data effectively.

Flame trajectory

For the jet trajectory in crossflow, early studies have proposed some scaling laws for determining jet trajectories. Karagozian [28] considers a vortex pair issuing from the jet orifice and into the crossflow, and numerical solution of the equations governing the evolution of this vortex pair gives the power law $z/d_j = \alpha r^{\beta}(x/d_j)^{\gamma}$ for the trajectory, where r is the momentum flux ratio, which is defined as $r = \sqrt{\rho_j u_j^2 / \rho_\infty u_\infty^2}$. Margarson [29] provided an extensive review of past work on jets in crossflow, found that the length scale rd_j can collapse the centerline trajectory of circular jets following the empirical relation $z/d_j = A(x/d_j)^B$, where A and B are constants. At present, the experimental values for A and B in many publications summarized by Margarson are different, and experimental results show $1.2 < A < 2.6$ and $0.28 < B < 0.34$. Hasselbrink and Mungal [30] assumed that $r^2 \gg 1$ and employed a similarity theory to treat the jet exit as a point source of momentum and intermediate asymptotic theory to scale the trajectory by length scale rd_j considering the entrainment

coefficients. Keffer and Baines [31] found that the trajectories collapse on normalizing the axes with $r^2 d_j$. However, all the above studies of jet trajectory are focused on the horizontal wind, and few studies have been done on the jet flame trajectory in upslope and downslope wind. In the upslope and downslope wind, distribution of velocity and scalar concentration may be changing, which may affect the evolution of the flame trajectory. Therefore, how would the flame trajectory change under upslope and downslope wind in the inclined tunnel?

Referring to the previous research [29-32] on the jet flow trajectory, d_j , rd_j and $r^2 d_j$ are often taken as the length scales for the jet trajectory. After a regression analysis, the jet flame trajectories determined from our experimental data for upslope wind and downslope wind are most satisfactory with the length scale $r^2 d_j$ following the empirical relation, as shown in Fig. 8, i.e.,

$$z/r^2 d_j = \alpha\left(x/r^2 d_j\right)^{0.875}, \tag{10}$$

where α is a constant.

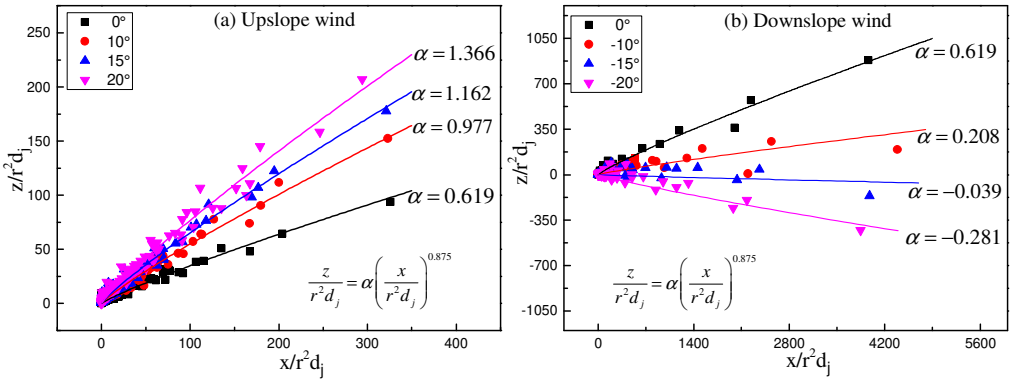

Fig. 8. Experimental results of flame trajectory under upslope and downslope wind.

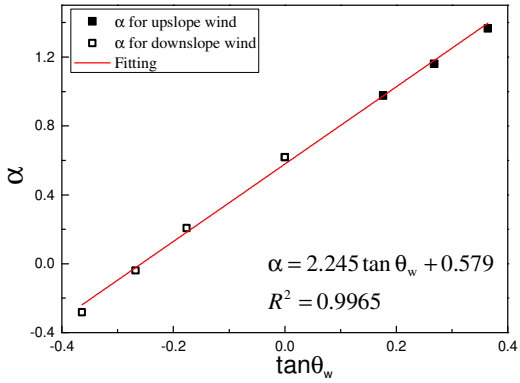

Fig. 9. Correlations of α under upslope and downslope wind.

Hasselbrink and Mungal [30] indicated that the air entrainment coefficient is directly related to the jet trajectory, and the jet is deflected entirely due to entrainment of crossflow fluid. When fuel jets burn in oblique wind, the rate at which the flame entrains and mixes a stoichiometric amount air is different from the rate in the crossflow. Thus, the jet trajectory would be affected by the rate of air entrainment. The air entrainment would change with the increasing of crossflow, and so would the orientation of the fuel jet relative to the air wind, which implies that α is correlated with the change of entrainment in the jet region with the change of wind attack angle. The linear relation between α and wind attack angles is shown in Fig. 9 for upslope and downslope wind,

$$\alpha = 2.245 \tan \theta_w + 0.579 . \quad (11)$$

Results show that the orientation of the fuel jet relative to the air wind has a consistent dependence on the change of entrainment, that is, with an increase in the wind attack angle θ_w, the constant α that is correlated with the entrainment increases for upslope wind and downslope wind.

CONCLUSIONS

Experimental investigations of the effects of wind attack angles on the characteristics of jet diffusion flames under upslope and downslope wind conditions have been conducted. The following conclusions can be drawn:

1) For upslope wind cases, as the wind attack angle increases, the phenomenon of flame downwash occurs at higher wind speeds than under horizontal flow. Flame downwash occurs for $u_w \geq 1.59$ m/s and $\theta_w = 0°$, while it occurs for $u_w = 2.12$ m/s when $\theta_w \geq 10°$. For downslope wind cases, the luminous zone base of the flame moves down along the lee sides of the nozzle at lower wind speeds ($u_w \geq 0.57$ m/s for $\theta_w \leq -10°$) than under horizontal flow ($u_w \geq 0.95$ m/s for $\theta_w = 0°$).

2) At a given attack angle for upslope and downslope wind, the flame tilt angle generally increases with the increase of wind speed up to an asymptotic value ($90° + \theta_w$). At a given wind speed, flame tilt decreases with the increase of wind attack angles.

3) The flame trajectory in the jet region shows different evolutionary trends under upslope and downslope wind, which can be collapsed by normalizing coordinates with the length scale $r^2 d_j$.

4) Two correlations are developed to predict the tilt angle and flame trajectory of the curved jet diffusion flames under upslope and downslope wind conditions, which obviously improve the prediction accuracy compared to previous models.

ACKNOWLEDGMENTS

The authors appreciate the support of the Natural Science Foundation of China (No. 51574210), Key national R & D program (No. 2016YFC0800603), and the open project program of the State Key Laboratory of Safety and Control for Chemicals (No. 10010104-15-ZC0613-0114).

REFERENCES

[1] R. Karagozian, Transverse jets and their control, Progr. Energy Combust. Sci. 36 (2010) 531–53.

[2] R. Camussi, G. Guj, A. Stella, Experimental study of a jet in a crossflow at very low Reynolds number, J. Fluid Mech. 454 (2002) 113-144.

[3] G. Heskestad, Turbulent Jet Diffusion Flames: Consolidation of Flame Height Data, Combust. Flame 118 (1999) 51-60.

[4] M.A. Delichatsios, Transition from Momentum to Buoyancy-Controlled Turbulent Jet Diffusion Flames and Flame Height Relationships, Combust. Flame 92 (1993) 349-364.

[5] T. Brzustowski, The hydrocarbon turbulent diffusion flame in subsonic cross-flow, 15th Aerospace Sciences Meeting; 1977, pp. 222.

[6] O.A. Pipkin, C.M. Sliepcevich, Effect of Wind on Buoyant Diffusion Flames. Initial Correlation, Ind. Eng. Chem. Fundam. 3.2 (1964) 147-154.

[7] J.R. Welker, O.A. Pipkin, C.M. Sliepcevich, The effect of wind on flames, Fire Technol. 1 (1965) 122-129.

[8] Y. Oka, O. Sugawa, T. Imamura, Y. Matsubara, Effect of cross-winds to apparent flame height and tilt angle from several kinds of fire source, Fire Safety Sci. 7 (2003) 915-926.

[9] J. Wang, J. Fang, S. Lin, et al., Tilt angle of turbulent jet diffusion flame in crossflow and a global correlation with momentum flux ratio, Proc. Combust. Inst. 36 (2017) 2979-2986.

[10] G.T. Kalghatgi, The visible shape and size of a turbulent hydrocarbon jet diffusion flame in a cross-wind, Combust. Flame 52 (1983) 91-106.

[11] D.M. De Faveri, A. Vidili, R. Pastorino, et al., Wind effects on diffusion flames of fires of high source momentum, J. Hazard. Mater. 22 (1989) 85-100.

[12] A.J. Majeski, D.J. Wilson, L.W. Kostiuk, Predicting the length of low-momentum jet diffusion flames in crossflow, Combust. Sci. Technol. 176 (2004) 2001-2025.

[13] Q. Wang, L. Hu, X. Zhang, et al., Turbulent jet diffusion flame length evolution with cross flows in a sub-pressure atmosphere, Energy Convers. Manage. 106 (2015) 703-708.

[14] P. Zhu, X.S. Wang, Y.P. He, et al., Flame characteristics and burning rate of small pool fires under downslope and upslope oblique winds, Fuel 184 (2016) 725-734.

[15] C. Tao, Y. He, Y. Li, X. Wang, Effects of oblique air flow on burning rates of square ethanol pool fires, J. Hazard. Mater. 260 (2013) 552–62.

[16] P. Zhu, X.S. Wang, C. Tao, Experiment study on the burning rates of ethanol square pool fires affected by wall insulation and oblique airflow, Exp. Therm. Fluid Sci. 61 (2015) 259–268.

[17] J.L. Ellzey, J.G. Berbe, E.Z.F. Tay, et al., Total soot yield from a propane diffusion flame in cross-flow, Combust. Sci. Technol. 71 (1990) 41-52.

[18] L. Orloff, J. De Ris, M.A. Delichatsios, Radiation from buoyant turbulent diffusion flames, Combust. Sci. Technol. 84 (1992) 177-186.

[19] G. Hankinson, B.J. Lowesmith, A consideration of methods of determining the radiative characteristics of jet fires, Combust. Flame 159 (2012) 1165-1177.

[20] M.R. Johnson, L.W. Kostiuk, Efficiencies of low-momentum jet diffusion flames in crosswinds, Combust. Flame 123 (2000) 189-200.

[21] L.W. Kostiuk, A.J. Mejeski, P. Poudenx, et al., Scaling of wake-stabilized jet diffusion flames in a transverse air stream, Proc. Combust. Inst. 28 (2000) 553-559.

[22] Y. Oka, H. Kurioka, H. Satoh, et al., Modelling of unconfined flame tilt in cross-winds, Fire Saf. Sci. 6 (2000) 1101-1112.

[23] G. Heskestad, Luminous heights of turbulent diffusion flames, Fire Saf. J. 5 (1983) 103-108.

[24] A. Kitajima, T. Ueda, A. Matsuo, et al., A comprehensive examination of the structure and extinction of turbulent non-premixed flames formed in a counterflow, Combust. Flame 121 (2000) 301-311.

[25] S.R. Turns, An introduction to combustion: concepts and applications, 3rd ed., McGraw-Hill, Boston, 2012.

[26] L. Hu, K. Lu, M.A. Delichatsios, L. He, F. Tang, An experimental investigation and statistical characterization of intermittent flame ejecting behavior of enclosure fires with an opening, Combust. Flame 159 (2012) 1178–84.

[27] N. Peters, Turbulent Combustion, Cambridge University Press, Cambridge, U.K., 2000, pp. 203.

[28] A.R. Karagozian, An analytical model for the vorticity associated with a transverse jet, AIAA J. 24 (1986) 429–436.

[29] R.J. Margason, 1993 Fifty years of jet in cross flow research, Report No. N94-28003 07-34, Winchester, UK, 1993.

[30] E.F. Hasselbrink, M.G. Mungal, Transverse jets and jet flames. Part 1. Scaling laws for strong transverse jets, J. Fluid Mech. 443 (2001) 1-25.

[31] J.F. Keffer, W.D. Baines, The round turbulent jet in a cross-wind, J. Fluid Mech. 15 (1963) 481-496.

[32] E.J. Gutmark, I.M. Ibrahim, S. Murugappan, Circular and noncircular subsonic jets in cross flow, Phys. Fluids 20 (2008) 075110.